

COMMUNICATION EFFICIENT APPLICATION OF SEQUENCES OF PLANAR ROTATIONS TO A MATRIX

THIJS STEEL* AND JULIEN LANGOU†

Abstract. We present an efficient algorithm for the application of sequences of planar rotations to a matrix. Applying such sequences efficiently is important in many numerical linear algebra algorithms for eigenvalues. Our algorithm is novel in three main ways. First, we introduce a new kernel that is optimized for register reuse in a novel way. Second, we introduce a blocking and packing scheme that improves the cache efficiency of the algorithm. Finally, we thoroughly analyze the memory operations of the algorithm which leads to important theoretical insights and makes it easier to select good parameters. Numerical experiments show that our algorithm outperforms the state-of-the-art and achieves a flop rate close to the theoretical peak on modern hardware.

Key words. High-performance computing, cache efficiency, BLAS, Givens rotations, eigenvalue computation

1. Introduction. The problem we will focus on in this paper is the application of a sequence of planar rotations to a matrix. A basic algorithm to apply such a sequence can be simple: we just loop over the rotations and apply each one to the matrix. Pseudocode for this algorithm is given in Algorithm 1.2 and our C implementation is not much more complicated.

Applying a sequence of orthogonal transformations efficiently is an important building tool in numerical linear algebra. To achieve high performance, many factorizations limit their initial calculations to a smaller submatrix of the original matrix. Updating the rest of the matrix (which often involves the bulk of the floating-point operations) can then be done efficiently with an optimized routine. The two most common orthogonal transformations are Givens rotations and Householder reflectors. Givens rotations are applied to two vectors (usually two columns or rows of a matrix) and are defined by a cosine and a sine. Householder reflectors can involve an arbitrary number of vectors. To apply a sequence of reflectors efficiently, the most popular method relies on the WY representation [8]. Through the use of this factorization, routines that apply a sequence of reflectors to a matrix can be optimized to achieve close to the theoretical peak flop rate on modern hardware. Because of this, reflectors have become the preferred choice for orthogonal transformations. However, some algorithms require the use of rotations. In case the matrix has a special structure (for example, if it is upper triangular), applying a reflector to it can destroy that structure. If rotations are used instead, the structure can more easily be preserved. Some examples are the implicit QR algorithm [3] and the Jacobi method for the singular value decomposition [5].

The basic algorithm presented in Algorithm 1.2 is not very efficient on modern hardware. The main reason for this is inefficient memory access because the algorithm is not cache-friendly. If we refer to the rotation whose values are stored in position (i, j) of the matrices C and S as rotation (i, j) , then we can say that column i of the matrix the rotations are applied to is involved in rotations $(i - 1, j)$ and (i, j) for all j . But in between applying (i, j) and $(i, j + 1)$, we need to load and store the entire matrix, so it is unlikely that the values of column i are still in the cache when we need them again. Kågström et al. [6] and later Van Zee et al. [10] have improved upon this basic algorithm in two ways, fused rotations and a wavefront pattern.

*KU Leuven, Belgium

†University of Colorado Denver, USA and Centre Inria de Lyon, France

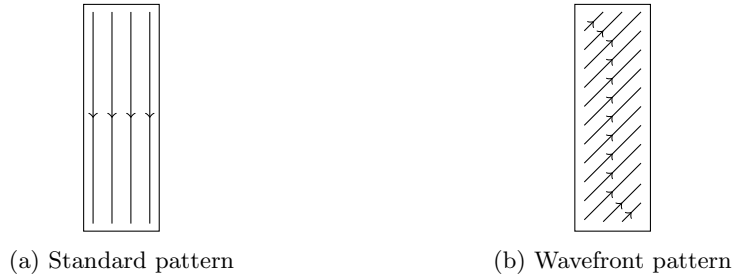


Fig. 1: The matrix C containing the cosines of the rotations and arrows indicating the order in which the rotations are applied. On the left, the standard pattern which applies full sequences of rotations. On the right, the wavefront pattern which applies the rotations in “waves”.

1.1. Wavefront algorithm. In the standard algorithm, we need to load and store the entire matrix between applying rotation (i, j) and $(i, j + 1)$. In an ideal world, we would just change the order of the loops so that rotation $(i, j + 1)$ is applied immediately after rotation (i, j) . Sadly, this is not allowed. Before we can apply rotation $(i, j + 1)$, we have to apply rotation $(i + 1, j)$. This leads to a wavefront pattern, where we apply rotation (i, j) , then $(i - 1, j + 1)$, $(i - 2, j + 2)$, \dots . Figure 1 shows this pattern visually; each of the diagonal sequences is called a wave. The advantage of this pattern is that instead of accessing $n - 1$ columns before a column is used again, this pattern accesses k columns. Typically, k is much smaller than n , so it is much more likely that the column can remain in the cache.

1.2. I/O complexity. If we assume a two-memory machine with a small cache of size S and a large memory, we want to quantify the number of memory movement (read and write) between the memory and the cache. This is called the I/O complexity problem.

Recent work on I/O lower bounds have led to techniques and tools to mechanically compute the I/O lower bounds of parametrized programs [7]. Using the IOLB tool on Algorithm 1.2 leads to a I/O lower bound of $\frac{mnk}{\sqrt{S}}$. Since the total number of operations of our code is $6mnk$, this means that the operational intensity is at most $6\sqrt{S}$.

A quick analysis of the wavefront algorithm explained in Section 1.1 goes as follows. We need to apply mnk Givens rotations. m_b and k_b such that $m_b k_b \leq S$ real such that a block of size m_b -by- k_b of A fits in cache. At each step of the wavefront algorithm, we need to read one column of size m_b , and write back one column of size m_b , and load $2k_b$ cosines and since that represent k_b rotations. In this step, we will be able to do $m_b k_b$ rotations. Forgetting start and end clean up code, we need to do (roughly) $\frac{mnk}{m_b k_b}$ steps. And so the I/O of the algorithm is $\frac{mnk}{m_b k_b} (2m_b + 2k_b)$. For $k_b = \sqrt{S}$ and $m_b = \sqrt{S}$ we get $\frac{4mnk}{\sqrt{S}}$. Since the total number of operations of our code is $6mnk$, this means that the operational intensity for the wavefront algorithm is $\frac{3}{2}\sqrt{S}$.

Two conclusions. First, we see that the ratio between an I/O lower bound for our problem and the wavefront algorithm is a factor 4. Second, we see that the operational intensity of our kernel is pretty good. (For comparison, the operational intensity of GEMM is \sqrt{S} .) Therefore there is potential to be able to hide I/O's and

reach GEMM-like performance.

We note that an analysis of the number of cache misses of the wavefront algorithm, a related problem, is done in [10, §4.2].

1.3. Fused rotations. Despite what the name suggests, fused rotations are not directly accumulated in any way. Instead, a fused rotation is a technique to increase register reuse. The advantage becomes clear when we study what happens when we apply two rotations to three vectors x , y , and z :

1. Load rotation 1 into registers
2. for $i = 0, 1, \dots, n$
3. load $x[i]$ and $y[i]$ into registers
4. apply rotation 1 to $x[i]$ and $y[i]$
5. store $x[i]$ and $y[i]$
6. Load rotation 2 into registers
7. for $i = 0, 1, \dots, n$
8. load $y[i]$ and $z[i]$ into registers
9. apply rotation 2 to $y[i]$ and $z[i]$
10. store $y[i]$ and $z[i]$

A fused rotation would change this to:

1. Load both rotations into registers
2. for $i = 0, 1, \dots, n$
3. load $x[i]$, $y[i]$, and $z[i]$ into registers
4. apply rotation 1 to $x[i]$ and $y[i]$
5. apply rotation 2 to $y[i]$ and $z[i]$
6. store $x[i]$, $y[i]$, and $z[i]$

This applies the exact same arithmetic operations, but only loads and stores $y[i]$ once instead of twice. This is important because memory operations are much more expensive than arithmetic operations on modern hardware. We can use fused rotations to fuse rotations (i, j) and $(i + 1, j)$ or rotations (i, j) and $(i - 1, j + 1)$. We refer to these as 2×1 fused rotations and 1×2 rotations, respectively. We can fuse even more rotations so long as we have enough registers to store all the values. On a typical CPU, it is optimal to use 2×2 fused rotations.

Algorithm 1.1 $\text{rot}(x, y, c, s)$

Apply a single rotation to two vectors.

Require: Vectors x and y of length m , scalars c and s

- 1: **for** ($i = 0; i < m; i++$) **do**
 - 2: $t = c \cdot x[i] + s \cdot y[i]$
 - 3: $y[i] = -s \cdot x[i] + c \cdot y[i]$
 - 4: $x[i] = t$
 - 5: **end for**
-

1.4. Structure of this paper. By combining fused rotations and the wavefront pattern, Van Zee et al. [10] were able to achieve close to the theoretical peak flop rate on their machine. However, since they published their paper, computer architectures have advanced and memory operations have become more expensive relative to floating point operations. In this paper, we will introduce several techniques to further reduce the number of memory operations so that the algorithm can achieve optimal flop rates even on modern machines. In Section 2, we will expand upon the wavefront

Algorithm 1.2 rot_sequence(A, C, S)

Apply a sequence of $(n - 1)k$ rotations, stored in C and S , to a matrix A from the right.

Require: Matrix A of size $m \times n$, matrices C and S of size $(n - 1) \times k$

```
1: for ( $p = 0; p < k; p++$ ) do
2:   for ( $j = 0; j + 1 < n; j++$ ) do
3:     rot( $A(:, j), A(:, j + 1), C(j, p), S(j, p)$ )
4:   end for
5: end for
```

Algorithm 1.3 rot_sequence_wavefront(A, C, S)

Apply a sequence of $(n - 1)k$ rotations, stored in C and S , to a matrix A from the right. Note: this algorithm assumes $k \leq n - 1$.

Require: Matrix A of size $m \times n$, matrices C and S of size $(n - 1) \times k$

```
1: for ( $p = 0; p < k - 1; p++$ ) {Startup phase} do
2:   for ( $l = 0, j = p; l < j + 1; ++l, --j$ ) do
3:     rot( $A(:, j), A(:, j + 1), C(j, p), S(j, p)$ )
4:   end for
5: end for
6: for ( $p = k - 1; p < n - 1; ++p$ ) {Pipeline phase} do
7:   for ( $l = 0; j = p; l < k; ++l, --j$ ) do
8:     rot( $A(:, j), A(:, j + 1), C(j, p), S(j, p)$ )
9:   end for
10: end for
11: for ( $p = n - k; p < n - 1; ++p$ ) {Shutdown phase} do
12:   for ( $l = 1; j = n - 2; l < k; ++l, --j$ ) do
13:     rot( $A(:, j), A(:, j + 1), C(j, p), S(j, p)$ )
14:   end for
15: end for
```

pattern and introduce a blocked version of the algorithm which can efficiently utilize the caches. In Section 3, we will introduce a new technique to improve register reuse. We will construct an efficient kernel that applies $n_r \times k_r$ rotations to m_r rows. Instead of keeping the rotations in registers and loading new values of the columns in each iteration, we will keep some of the values of the columns in registers and load new rotations in each iteration. We will show that this significantly reduces the amount of memory operations.

2. Blocking. Blocking is a commonly used technique to improve cache utilization. Instead of working on a large matrix that does not fit into cache, we split the algorithm into smaller pieces. Those smaller pieces will involve smaller matrices that do fit into the cache, improving cache utilization.

The original algorithm applies k sequences of $n - 1$ rotations to m rows of a matrix. However, we cannot just split the algorithm into rectangular blocks that apply k_b sequences of n_b rotations to m_b rows. This is because of the same application order restrictions that led to the wavefront pattern. Inspired by the wavefront algorithm, we will instead split the algorithm into blocks that apply n_b waves of k_b rotations to m_b rows. Figure 3 shows how the matrices are split into blocks and Algorithm 2.1

shows an example implementation of such a block. Even now that the rotations are split into blocks, we still need to respect the order in which the rotations are applied. We need to apply the block starting at (i_b, j_b, p_b) before we can apply the block at $(i_b, j_b + n_b, p_b)$ or the block at $(i_b, j_b - k_b, p_b + k_b)$. This mostly has consequences when we will parallelize the code. It is also noteworthy that while most of the blocks are parallelograms, some blocks are triangular. These correspond to the startup and shutdown phases of the wavefront algorithm.

In Section 5, we will discuss the order in which we should treat the blocks and select the block sizes. But first, we will discuss how to implement the block.

Algorithm 2.1 `rot_sequence_block(A, C, S)`

Apply $n - k$ waves of k rotations, stored in C and S , to a matrix A from the right. This is one block of the blocked algorithm. Note how this algorithm does not have a startup or shutdown phase.

Require: Matrix A of size $m \times (n + k)$, matrices C and S of size $(n + k - 1) \times k$

- 1: **for** ($p = 0; p < k; p++$) **do**
 - 2: **for** ($j = k - 1 - p; j < n - p; j++$) **do**
 - 3: `rot(A(:, j), A(:, j + 1), C(j, p), S(j, p))`
 - 4: **end for**
 - 5: **end for**
-

3. A kernel for register reuse. In the previous section, we discussed how to split the algorithm into blocks to improve cache utilization. In this section, we will explain how to implement those small blocks efficiently. Just like in the previous section, our main focus will be reducing the cost of the memory operations, but instead of improving cache utilization, we will focus on improving register reuse.

Algorithm 2.1 implements one of the small blocks. If we count the number of memory operations needed, we see that we need $2m_b(n_b - k_b)k_b$ loads and stores for the values in A , and $2(n_b - k_b)k_b$ loads for the values in C and S or

$$(3.1) \quad 4m_b(n_b - k_b)k_b + 2(n_b - k_b)k_b \text{ memory operations.}$$

In this calculation, we assume the values of C and S are loaded into registers once and then reused for an entire rotation.

Using 2×2 fused rotations, we can reduce the number of memory operations to

$$(3.2) \quad 2m_b(n_b - k_b)k_b + 2(n_b - k_b)k_b \text{ memory operations.}$$

The more rotations we can fuse, the more we can reduce the number of memory operations. If we use $n_r \times k_r$ fused rotations, we can reduce the number of memory operations to

$$(3.3) \quad \left(\frac{2}{n_r} + \frac{2}{k_r} + \frac{2}{m_b}\right)m_b(n_b - k_b)k_b \text{ memory operations.}$$

Unfortunately, these fused rotations also require us to fit $2n_r k_r + k_r + n_r$ values in registers (and we also need at least one register as temporary storage to perform the rotation). On the CPUs we are targeting, we have 16 vector registers, so the largest fused rotation we can use is 2×2 .

To reduce the number of memory operations further, we need a different approach. We have mentioned before that we reuse the values of C and S by keeping them in

registers. In a 2×2 kernel, we can reuse 8 registers, while we only need to load and store 6 registers worth of data in A . On modern CPUs, we can use vector registers, which can store multiple values. On our machine, we can store 4 double-precision values in one vector register. An implementation detail when using vector registers and instructions is that we need to broadcast the values of C and S to registers, i.e. the registers that contain cosines and sines do not contain 4 different cosines and sines, but the same cosine and sine repeated 4 times. If we then look once again at the memory reuse, we see that 8 values of C and S can be reused, while 24 values of A need to be loaded and stored. This ratio becomes even worse when using single precision and/or 512-bit AVX registers. In the design of our kernel, we will try to reuse values of A instead of C and S .

Our kernel will apply n waves of k_r rotations to m_r rows of A . One wave touches $k_r + 1$ columns of A , of which k_r can be reused for the next wave of rotations. The number of memory operations needed for one block is now

$$(3.4) \quad \left(\frac{2}{k_r} + \frac{2}{n_b} + \frac{2}{m_r}\right)m_b(n_b - k_b)k_b \text{ memory operations.}$$

This equation is similar to Equation (3.3) so it may seem that we have not improved the number of memory operations, but the key is that m_r can be much larger than 2. Assuming we have 16 256-bit AVX registers and are working in double precision, we can choose $m_r = 8$ and $k_r = 5$. If n_b is sufficiently large, this will reduce the number of memory operations to

$$(3.5) \quad 0.65m(n - k)k \text{ memory operations.}$$

This is a factor 3 improvement over the $2m(n - k)k$ memory operations needed by the 2×2 fused rotations. We will later show in the experiments that a kernel with $m_r = 16$, $k_r = 2$ performs slightly better, despite requiring more memory operations than the $m_r = 8$, $k_r = 5$ kernel.

We could also have chosen to construct a kernel that applies a sequence of n_r rotations to m_r rows of A . This would have resulted in a similar number of memory operations and similar kernel sizes.

4. Packing. In the previous sections, we split the algorithm into smaller blocks to allow for better cache locality and we also rearranged the inner loop to allow for more register reuse. However, both of these optimizations have the effect of making the memory accesses less contiguous. Among other reasons, accessing memory in a contiguous way is important because of cache lines and the translation lookaside buffer (TLB).

4.1. Cache lines. When we access an element from the main memory, that element is put into the cache in case we need it again later. However, the cache does not track individual elements, but rather cache lines. These are blocks of typically 64 contiguous bytes. If we access an element, the entire cache line is loaded into the cache. If we then access another element in the same cache line, we can get it directly from the cache, which is much faster than getting it from the main memory. When incrementing i first, we access the elements of A in a contiguous way, which almost guarantees that each cache line will be fully utilized. When incrementing j or p first, we only access m_r values of A in a contiguous way before we move on to the next column of A , which is almost certainly in a different cache line¹.

¹If the matrix is properly aligned to a cache line boundary, its leading dimension is a multiple of the cache line size and m_r is also a multiple of the cache line size, then the cache lines will still be

4.2. TLB. An important component of computer architectures that we have not yet taken into account is virtual memory. If you allocate space for a large matrix, you can write your program as if the matrix is stored in a contiguous block of memory, but in reality, the memory is fragmented into chunks called pages. Pages are typically 4kb. Programmers typically do not need to worry about translating the virtual (contiguous) memory addresses to the physical (fragmented) memory addresses because the operating system takes care of this for you. However, it is important to remember that this translation involves looking up the physical address in the page table. As mentioned before, memory lookups are slow, so just as recently used entries of the matrix are stored in a cache, recently used entries of the page table are stored in the TLB. If the matrix is large enough so that subsequent columns of A are in different pages and there are not enough TLB entries to track all the columns of A , then every m_r accesses of A will incur a TLB miss.

4.3. Packing. In their discussion of high-performance matrix-matrix multiplications, Kazushige Goto et al. [4] discussed these issues and introduced the concept of packing. The idea is to make a “packed” copy of the matrix. Instead of being stored in column- or row-major order, this packed copy is stored in the exact way that it will be accessed. This way, they can fully utilize the cache lines and avoid TLB misses.

We can apply the same trick to our algorithm. We make a packed copy of A , apply the rotations to the packed copy, and then copy the result back to A . Figure 2 illustrates the packed format. We could also pack the matrices C and S , but this is less important. If we are applying a large number of rotations, the cost of packing and unpacking the matrix is negligible. However, if we are applying only a few rotations, the cost of packing and unpacking the matrix can be significant. If the algorithm is to be applied to the same matrix multiple times, it may be necessary to keep the matrix A in packed format instead of repacking on each call.

An extra advantage of packing is that we can make sure the packed matrix is aligned to a cache line boundary even if the original matrix is not. This is not only important for cache lines but also for SIMD instructions. Similarly, if we want to apply rotations from the left instead of from the right (or equivalently, apply rotations from the right to a row-major matrix), we can make sure that the accesses are contiguous in the packed matrix.

An important consideration is when to pack and unpack the matrix. To truly have sequential memory accesses, we should pack and unpack each block. However, the blocks have a lot of overlap, so we would be packing and unpacking the same values multiple times. Instead, we pack an entire $m_b \times n$ row-block of A . This leads to some strided accesses but avoids repacking.

5. Loop orders and choosing block sizes. We have discussed kernel design and blocking, but we have not discussed the order of the loops around the kernel and blocks. In this section, we will decide on the loop order and derive some formulas to choose good block sizes for the blocked algorithm. Instead of minimizing the number of cache misses at all levels of the memory hierarchy, we will instead maximize the number of values that are reused at each cache level. Specifically, we will choose n_b to optimize the L1 cache utilization, k_b to optimize the L2 cache utilization, and m_b to optimize the L3 cache utilization. We will specifically optimize for the $m_r = 16$, $k_r = 2$ kernel.

fully utilized.

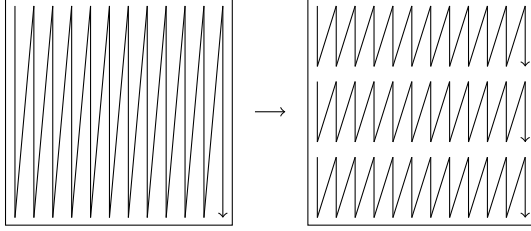


Fig. 2: Illustration of packing for the matrix A . The matrix on the left is stored in column-major order, the matrix on the right is stored in packed order.

5.1. The kernel. At the lowest level of the algorithm, we have the kernel. This kernel applies n_b waves of k_r rotations to m_r rows of the matrix. This involves a block of size $m_r(n_b + k_r)$ for A and of size $n_b k_r$ for C and S . Depending on the loop order, either the values of A or the values of C and S will be reused, so ideally, these blocks should fit into the L1 cache. We require all three blocks to fit into the L1 cache even though not all values will be reused to avoid evicting the wrong values from the cache. For maximum reuse, we should choose n_b as large as possible.

If we assume the L1 cache can fit T_1 floats, then we need to solve the following equation for n_b :

$$(5.1) \quad m_r(n_b + k_r) + 2n_b k_r \leq T_1.$$

$$(5.2) \quad \Rightarrow n_b \leq \frac{T_1 - m_r k_r}{m_r + 2k_r}.$$

On our machine, $T_1 = 4000$, so $n_b \leq 220$. To leave some room for other values, we will choose $n_b = 216$.

Note, if we had designed our kernel differently so that it applies sequences of n_r rotations instead of a wave of k_r rotations, we would have optimized k_b instead of n_b for the L1 cache and ended up with a similar equation. However, it is common to apply the full algorithm with large m and n , but small k . This is for example the case when applying delayed sequences of rotations in the implicit QR algorithm. If k is smaller than k_b , we will not be able to fully utilize the cache.

5.2. First loop around the kernel. The next level of the algorithm is the first loop around the kernel. If we choose to apply the same rotation to other rows of A , we can reuse $2n_b k_r$ values of C and S . If we choose to apply a different set of rotations, we can reuse $m_r n_b$ values of A . Which order leads to more reuse depends on the size of the kernel. Typically, m_r is going to be larger than $2k_r$, so we will choose to reuse values of A over values of C and S . This also makes the packing of A easier.

The loop now applies the kernel $\frac{k_b}{k_r}$ times. Because of the overlap between the blocks, most of the values of A are reused and remain in the L1 cache. To choose k_b , we will make sure that the bigger $m_r(n_b + k_b)$ block of A and $n_b k_b$ blocks of C and S fit into the L2 cache. If we assume the L2 cache can fit T_2 floats, then we need to solve the following equation for k_b :

$$(5.3) \quad m_r(n_b + k_b) + 2n_b k_b \leq T_2.$$

$$(5.4) \quad k_b \leq \frac{T_2 - m_r n_b}{m_r + 2n_b}.$$

Note that this equation depends on n_b , which also explains why we chose n_b first. On our machine, $T_2 = 32000$, so $k_b \leq 62$. We will choose $k_b = 60$.

5.3. Second loop around the kernel (full block). The next level of the algorithm is the second loop around the kernel, where we will apply the rotations to the next rows of A . The block of A expands from $m_r(n_b + k_b)$ to $m_b(n_b + k_b)$. We will make sure that this bigger block fits in the L3 cache. If we assume the L3 cache can fit T_3 floats, then we need to solve the following equation for m_b :

$$(5.5) \quad m_b(n_b + k_b) \leq T_3.$$

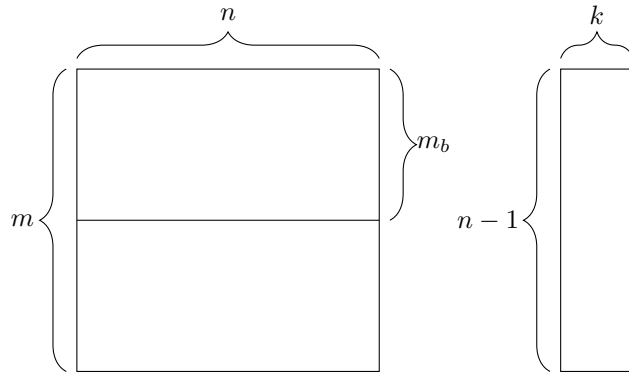
$$(5.6) \quad m_b \leq \frac{T_3}{n_b + k_b}.$$

On our machine, $T_3 = 4480000$, so $m_b \leq 16231$. We will choose a much smaller value because the L3 cache is shared between all cores and we want to avoid interfering with other processes. We will choose $m_b = 4800$.

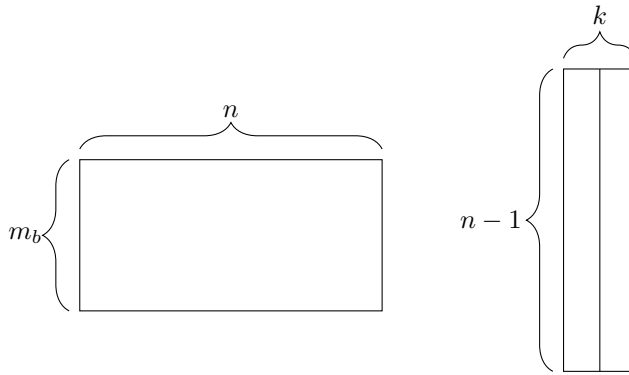
5.4. Loops around the blocks. We could similarly select the order of the loops around the blocks to optimize the memory cost. However, we will choose the order of these loops with an eye towards practical implementations. For the outer loop, we choose the loop over i (the row blocks of A). This is because it makes the algorithm easier to parallelize. For the second loop around the blocks, we choose p (the column blocks of C and S) because of the startup and shutdown phases. If we split k into blocks of k_b first, we need to do $\frac{k}{k_b}$ startup and shutdown phases of size $k_b \times k_b$, otherwise, we need to do one startup and shutdown phase of size $k \times k$, which would mean more work is done in the startup and shutdown phases. In principle, the startup and shutdown phases can be implemented just as efficiently as the pipeline phase, but it does require more effort from the programmer. By splitting k into blocks of k_b first, we can get away with a simpler implementation.

6. Reducing the number of operations. In this paper, we have focused on reducing the memory cost of applying a sequence of Givens rotations. In the literature, there have also been attempts to reduce the number of floating point operations. Normally, applying a rotation involves 4 multiplications and 2 additions. By keeping track of a scaling factor throughout the algorithm, it is possible to reduce this to 2 multiplications and 2 additions. This is called a modified or fast Givens rotation [1]. We will refer to the paper for the details of the algorithm. What is important for our purposes is that even though the modified Givens rotations involve fewer flops, they do require a branch. On modern architectures, with deep pipelines, branches can be very expensive.

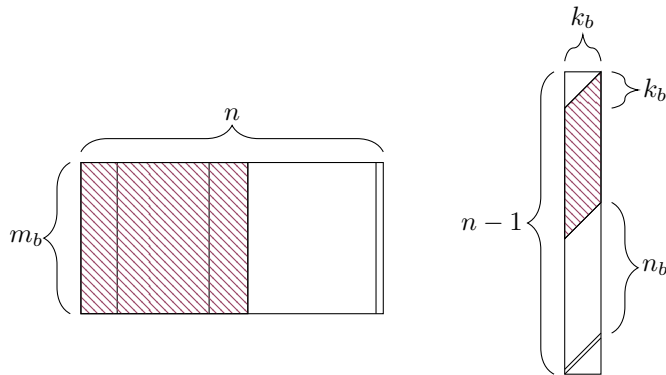
Alternatively, we can use 2x2 reflectors instead of rotations. A 2x2 reflector can fulfill the same role as a rotation, but it involves 3 multiplications and 3 additions. This is just as many flops as applying a rotation (6 flops), but it is still advantageous because multiplications are typically more expensive than additions. Additionally, modern architectures typically include fused-multiply-add instructions (FMA) that are faster than separate multiply and add instructions. Naturally, these instructions can only be used when the number of multiplications is equal to the number of additions. Despite their ability to use FMA instructions effectively, we will show in Section 8 that our implementation of the reflectors is actually slower than the implementation of the rotations. Further research will be needed to determine the cause.



(a) Third loop around the blocks (full algorithm)



(b) Second loop around the blocks



(c) First loop around the blocks

Fig. 3: Illustration of the blocking scheme. On the left, the matrix A to whose columns the rotations are applied, and on the right, the matrix C containing the cosines of the rotations. We do not show the matrix S here because its blocks are identical to those of C . One of the blocks is indicated with diagonal lines. Notice how that block covers two of the rectangles in A : the blocks in A overlap.

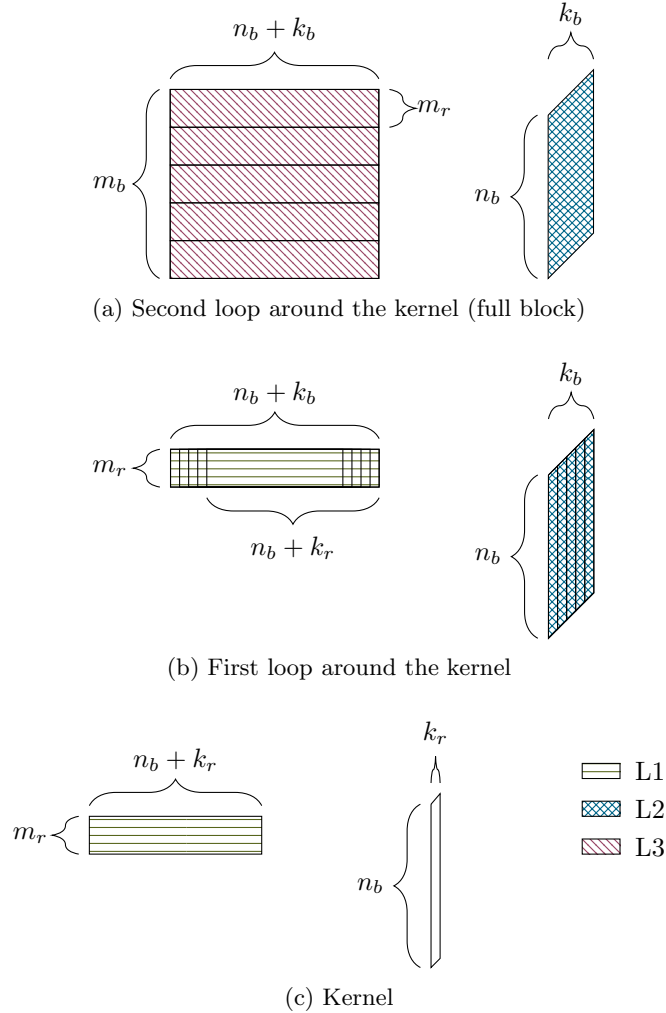


Fig. 4: Illustration of the application of a block of rotations using the kernel. On the left, the matrix A to whose columns the rotations are applied, and on the right, the matrix C containing the cosines of the rotations. We do not show the matrix S here because its blocks are identical to those of C .

7. Parallelization. There are two places where we can parallelize the algorithm. The first is the loop over i_b , the second is the loop over i . The other loops cannot easily be parallelized.

When parallelizing, we need to take into account which of the caches are shared. If the L2 cache is shared, we may need to reduce k_b to avoid interference between the different cores. The L3 cache being shared is not a problem if we parallelize over i , but if we parallelize over i_b , we may need to reduce m_b to avoid interference.

Finally, we also need to make sure the load is balanced between the different cores. Instead of using a fixed blocksize m_b , we can use $\frac{m}{n_{threads}}$, rounding up to the

nearest multiple of m_r . This way, the load is balanced between the different cores.

8. Experiments. In this final section, we test the performance of the different algorithms on two different machines. We will compare the following algorithms:

- `rs_unoptimized`: The naive algorithm to apply a rotation sequence described in Algorithm 1.2.
- `rs_blocked`: Uses blocks as described in Section 2, but does not use the kernel described in Section 3.
- `rs_fused`: The algorithm described in [10]. It uses 2×2 fused rotations whenever possible (including in the startup and shutdown phases).
- `rs_gemm`: Instead of applying the rotations directly, this algorithm accumulates blocks of rotations into orthogonal matrices using 2×2 fused rotations and applies those using DGEMM and DTRMM from MKL. Note: this algorithm requires more flops than the other algorithms. When reporting the flop rate, we will only count the flops required to apply the rotations.
- `rs_kernel`: The algorithm described in this paper. It uses an $m_r = 16$, $k_r = 2$ kernel, but switches to an $m_r = 16$, $k_r = 1$ kernel to apply the startup and shutdown phases².
- `rs_kernel_v2`: Same as `rs_kernel`, but the matrix A is already in packed format before the algorithm is called.

The algorithms are implemented in C and are (where applicable) parallelized using OpenMP. The experiments are run on two different machines:

- Xeon V2: this machine has two Intel Xeon E5-2650 v2 processors, each of which has 8 cores. These processors support AVX instructions but do not have FMA instructions. At the base clock rate, this machine has a peak single-core double precision flop rate of 20.8 Gflop/s. At the maximum clock rate, the flop rate increases to 27.2 Gflop/s.
- Xeon V3: this machine has two Intel Xeon E5-2697 v3 processors, each of which has 14 cores. These processors support AVX2 instructions and FMA instructions. At the base clock rate, this machine has a peak single-core double precision flop rate of 41.6 Gflop/s. At the maximum clock rate, the flop rate increases to 54.4 Gflop/s.

8.1. Serial performance. We first test the performance of the different algorithms on a single core. We apply the algorithms with $k = 180$, varying n and $m = n$. The results are shown in Figure 5. The first thing to notice is that the blocked version and the unoptimized version achieve about the same flop rate for small matrices, but because of poor cache utilization, the performance of the unoptimized version quickly drops for even moderately sized matrices. The blocked version, on the other hand, maintains a high flop rate for all n . The version with 2×2 fusing is approximately 30% faster than the blocked version for all n . F. Van Zee et al. [10] reported that their fused version was 50% faster than the blocked version on their machine. The difference between the two speedups is likely because they tested their algorithm on a different machine. It is also interesting to see that for large matrices, `rs_gemm` outperforms `rs_fused`. The poor performance of `rs_gemm` for small matrices shows that the accumulation of the rotations can be an important bottleneck. This would likely be even more pronounced in a parallelized version. Finally, we can see that the kernel version is about 60% faster than the blocked version and between 20 and 30% faster

²It is also possible to use a modified $m_r = 16$, $k_r = 2$ kernel for large parts of the startup and shutdown phases, we just did not implement this because of time constraints.

than the fused version for all n . We also see that `rs_kernel_v2` is noticeably faster than `rs_kernel` for large matrices. Even though the difference is small, it is likely worth the effort to keep the matrix in packed format if possible. Finally, we see that on the Xeon V2, the flop rate of the kernel version is close to the theoretical peak flop rate of the machine. On the Xeon V3, we do not reach the peak flop rate, but we do get closer than with the other algorithms.

8.2. Selecting kernel size. In `rs_kernel`, we have chosen the kernel of size $m_r = 16$, $k_r = 2$. We will now test the performance of the algorithm for different kernel sizes, which will show that this kernel is the fastest. Since the block sizes m_b , k_b , and n_b are also dependent on the size of the kernel, we have tuned different block sizes for each kernel size and use those in the experiments. The results are shown in Figure 6. We see that the $m_r = 16$, $k_r = 2$ is indeed the fastest, although the difference with the $m_r = 12$, $k_r = 3$ kernel is small. A small note here is that we did not fully optimize the startup and shutdown phases. In those phases, we revert to a kernel with $k_r = 1$, which means that there is a small bias toward kernels with small k_r . It may well be that the $m_r = 12$, $k_r = 3$ kernel performs better if the startup and shutdown phases are fully optimized. It is also noteworthy that according to Equation (3.4), the $m_r = 16$, $k_r = 2$ kernel needs almost twice as many memory operations as the $m_r = 8$, $k_r = 5$ kernel. We do not currently have a satisfying explanation as to why it is still faster.

8.3. Parallel performance. Next, we test the performance of the `rs_kernel_v2` on multiple cores. We use the same parameters as before $k = 180$, varying n and $m = n$. We have parallelized our code around the outer loop (i_b). The results are shown in Figure 7. The first thing to notice is that the speedup is quite good. For the Xeon V2, we get a speedup of about 10 for 16 threads. For the Xeon V3, we get a speedup of about 16 for 28 threads. The high parallel efficiency is expected because the communication between threads is limited. The threads apply the same rotations to different rows of A . The second thing to notice is that while the flop rate of the serial code is fairly independent of n , the flop rate of the parallel code goes up and down. This is because of load balancing. For the kernel to work, we need to have a multiple of m_r rows in each block. That means that if we want each thread to handle the same number of rows, we need m to be a multiple of m_r times the number of threads. The peaks in the flop rate are where this is the case. A possible solution is to make a smaller kernel to handle the edge cases.

8.4. Performance of 2x2 reflectors. Finally, we look at the performance of the different algorithms if they are modified to apply 2x2 reflectors instead of Givens rotations. We use the same parameters as before: $k = 180$, varying n and $m = n$. The fused algorithm still uses 2x2 fusing, but the size of the kernel is reduced to $m_r = 12$, $k_r = 2$. The results are shown in Figure 8. Even though our kernel algorithm is still faster than the other algorithms, it is clear that switching to 2x2 reflectors negatively impacted the performance. We emphasize that we do not believe that this indicates a fundamental issue with using reflectors, but it is rather an indication that further research will be required to unlock the full potential of the reflectors.

9. Conclusion. We have presented a new algorithm to apply sequences of rotations to a matrix. We have shown that our algorithm is faster than the state-of-the-art and achieves close to the theoretical limits of the hardware. We have also shown that our algorithm scales well to multiple cores.

In the conclusion of their paper on the wavefront algorithm, F. G. Van Zee et

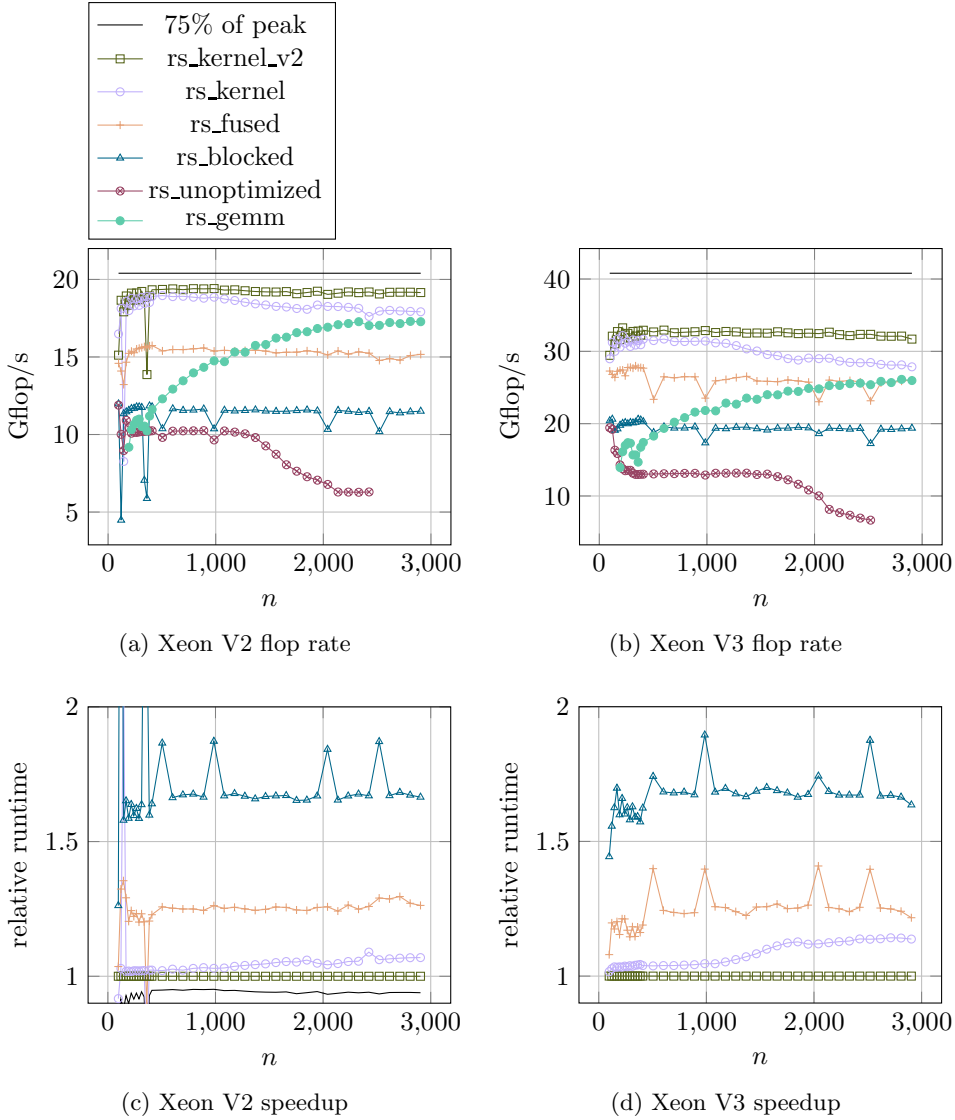


Fig. 5: On top, the Flop rates of the different algorithms. On the bottom, the runtime of the different algorithms relative to rs_kernel_v2.

al. [10] noted that their work may result in a renaissance for the implicit QR algorithm. Although these hopes did not fully materialize in the 10 years since then, we believe that our work represents another chance for the implicit QR algorithm. In future work, we will

- Push for the inclusion of rotation sequences in the BLAS [2]. Additionally, we will contribute our optimized implementation to BLIS [9]. We believe that only through easy access to highly optimized implementations, other researchers will be able to take advantage of our work.

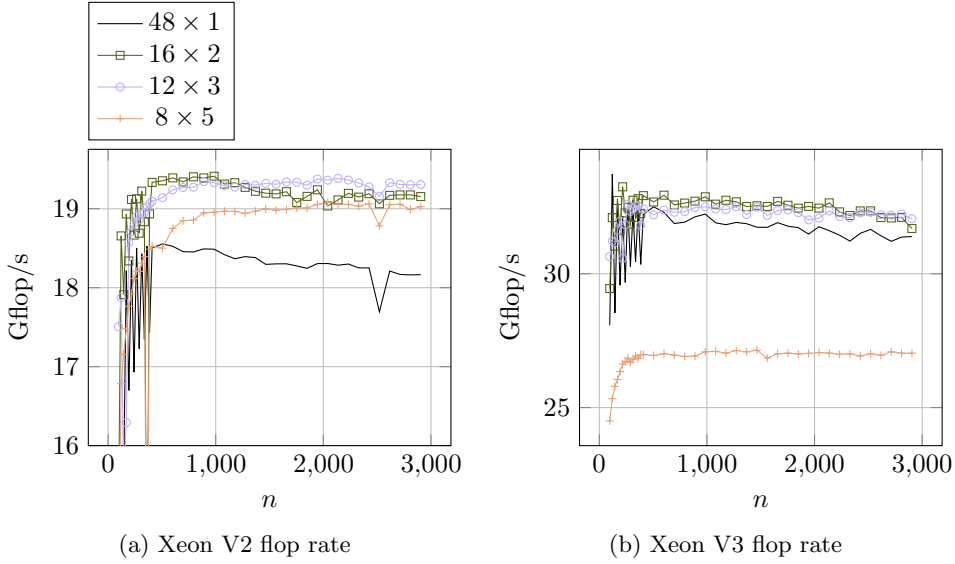


Fig. 6: Performance of `rs_kernel_v2` for different block sizes.

- Investigate the performance of our algorithm on other architectures. It should be easy to implement an efficient kernel for more recent CPUs with AVX512 support, but we are also interested in extending the algorithm to GPUs and distributed systems.
- Modify existing methods, such as the implicit QR algorithm, to take advantage of our algorithm. This may present new challenges, such as the need to handle 3x3 reflectors for the double-shift Hessenberg QR algorithm.

Acknowledgments. Julien was partially supported for this work by NSF award #2004850.

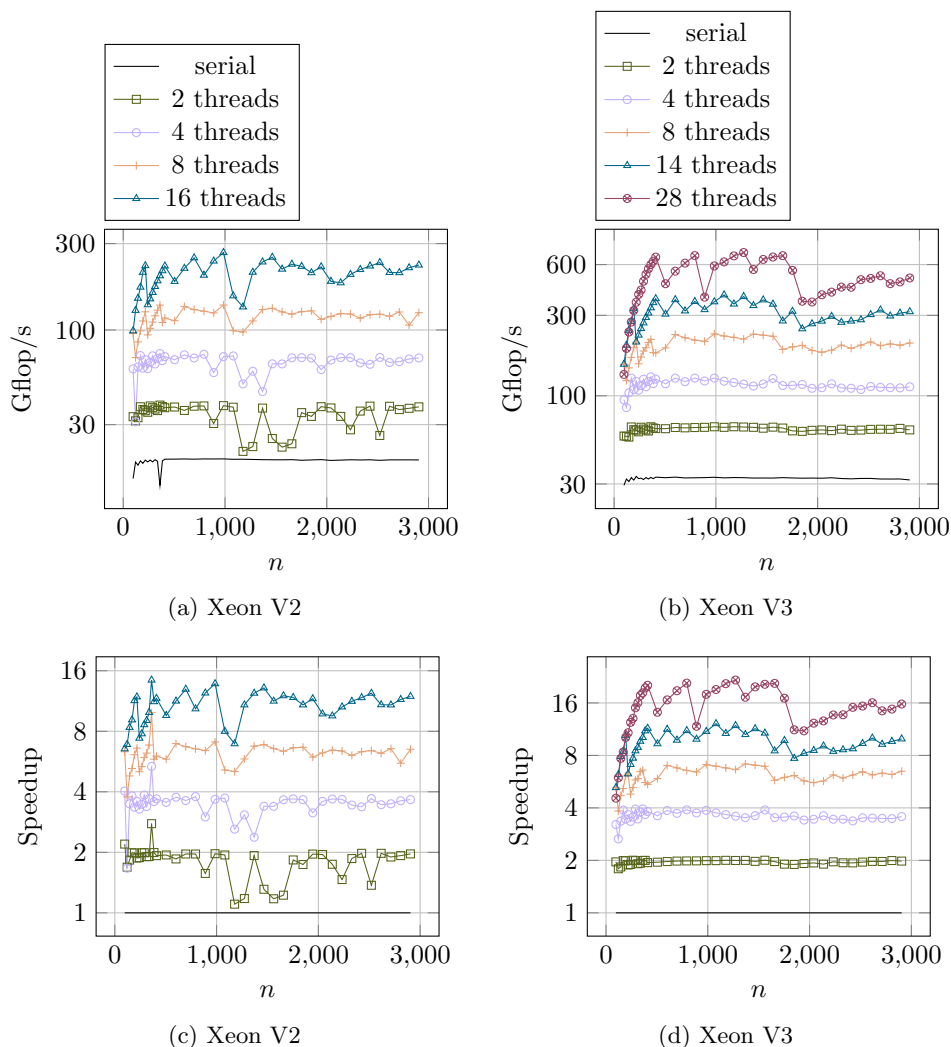


Fig. 7: On top: the flop rates of `rs_kernel_v2` using a varying amount of threads. On the bottom: the speedup of the parallel versions relative to the serial version.

REFERENCES

- [1] A. A. ANDA AND H. PARK, *Fast plane rotations with dynamic scaling*, SIAM Journal on Matrix Analysis and Applications, 15 (1994), pp. 162–174.
- [2] J. J. DONGARRA, J. DU CROZ, S. HAMMARLING, AND I. S. DUFF, *A set of level 3 basic linear algebra subprograms*, ACM Transactions on Mathematical Software (TOMS), 16 (1990), pp. 1–17.
- [3] J. G. FRANCIS, *The QR transformation a unitary analogue to the LR transformation—part 1*, The Computer Journal, 4 (1961), pp. 265–271.
- [4] K. GOTO AND R. A. V. D. GEIJN, *Anatomy of high-performance matrix multiplication*, ACM Transactions on Mathematical Software (TOMS), 34 (2008), pp. 1–25.
- [5] C. G. J. JACOBI, *Über ein leichtes verfahren die in der theorie der säcularstörungen vorkommenden gleichungen numerisch aufzulösen*, Journal für die reine und angewandte Mathe-

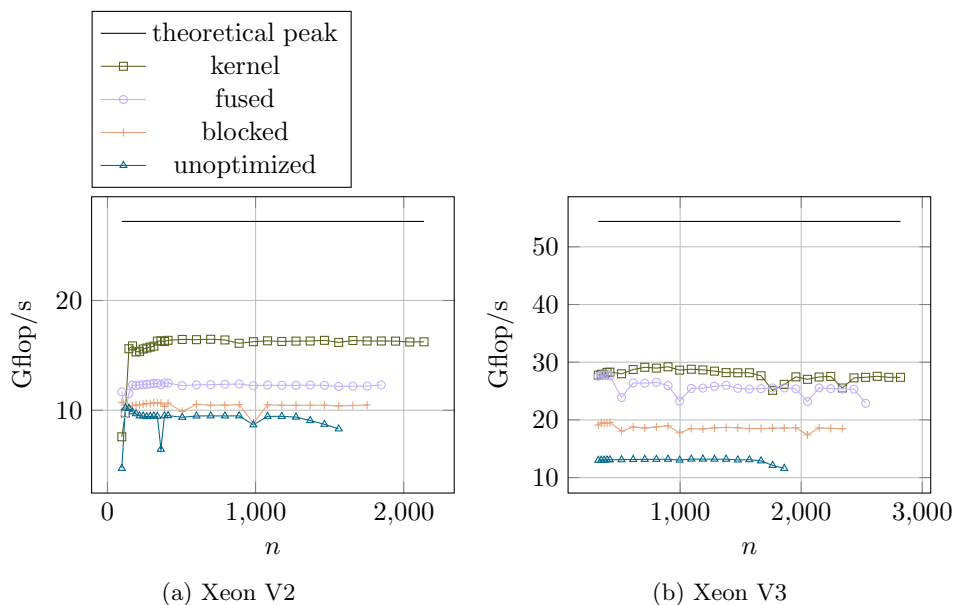


Fig. 8: Flop rates of different algorithms to apply a sequence of 2×2 reflectors to a matrix. The theoretical peak flop rate is 100% of the peak flop rate at the maximum frequency.

- matik, (1846).
- [6] B. KÄGSTRÖM, D. KRESSNER, E. S. QUINTANA-ORTÍ, AND G. QUINTANA-ORTÍ, *Blocked algorithms for the reduction to Hessenberg-triangular form revisited*, BIT Numerical Mathematics, 48 (2008), pp. 563–584.
 - [7] A. OLIVRY, J. LANGOU, L.-N. POUCHET, P. SADAYAPPAN, AND F. RASTELLO, *Automated derivation of parametric data movement lower bounds for affine programs*, in Proceedings of the 41st ACM SIGPLAN Conference on Programming Language Design and Implementation, PLDI 2020, ACM New York, NY, USA, 2020, pp. 808–822.
 - [8] R. SCHREIBER AND C. VAN LOAN, *A storage-efficient WY representation for products of Householder transformations*, SIAM Journal on Scientific and Statistical Computing, 10 (1989), pp. 53–57.
 - [9] F. G. VAN ZEE AND R. A. VAN DE GEIJN, *BLIS: A framework for rapidly instantiating BLAS functionality*, ACM Transactions on Mathematical Software, 41 (2015), pp. 14:1–14:33, <https://doi.acm.org/10.1145/2764454>.
 - [10] F. G. VAN ZEE, R. A. VAN DE GEIJN, AND G. QUINTANA-ORTÍ, *Restructuring the tridiagonal and bidiagonal QR algorithms for performance*, ACM Transactions on Mathematical Software (TOMS), 40 (2014), pp. 1–34.